Journal of
Micro/Nanolithography, MEMS, and MOEMS

SPIEDigitalLibrary.org/jm3

Thermomechanical design, hybrid fabrication, and testing of a MOEMS deformable mirror

Claudia Reinlein
Michael Appelfelder
Sylvia Gebhardt
Erik Beckert
Ramona Eberhardt
Andreas Tünnermann

SPIE

Thermomechanical design, hybrid fabrication, and testing of a MOEMS deformable mirror

Claudia Reinlein
Michael Appelfelder
Friedrich Schiller University of Jena
Institute of Applied Physics
Fraunhofer Institute for Applied Optics and Precision Engineering
Albert-Einstein-Straße 7
07745 Jena, Germany
E-mail: claudia.reinlein@iof.fraunhofer.de

Sylvia Gebhardt
Fraunhofer Institute for Ceramic Technologies and Systems IKTS
Winterbergstraße 28
01277 Dresden, Germany

Erik Beckert
Ramona Eberhardt
Fraunhofer Institute for Applied Optics and Precision Engineering
Albert-Einstein-Straße 7
07745 Jena, Germany

Andreas Tünnermann
Friedrich Schiller University of Jena
Institute of Applied Physics
Fraunhofer Institute for Applied Optics and Precision Engineering
Albert-Einstein-Straße 7
07745 Jena, Germany

Abstract. This paper reports on the thermomechanical modeling and characterization of a micro-opto-electro-mechanical systems deformable mirror (DM). This unimorph DM offers a low-temperature cofired ceramic substrate with screen-printed piezoceramic actuators on its rear surface and a machined copper layer on its front surface. We present the DM setup, thermomechanical modeling, and hybrid fabrication. The setup of the DM is transferred into a thermomechanical model in ANSYS Multiphysics. The thermomechanical modeling of the DM evaluates and optimizes the mount material and the copper-layer thickness for the loading cases: homogeneous thermal loading and laser-loading of the mirror. Subsequently, the developed and theoretically optimized DM setup is experimentally validated. The homogeneous loading of the optimized design results in a membrane deformation with a rate of $-0.2\ \mu m\,K^{-1}$, whereas the laser loading causes an opposed change with a rate of $-0.2\ \mu m\,W^{-1}$. Therefore, the proposed mirror design is suitable to precompensate laser-generated mirror deformations by homogeneous thermal loading (heating). We experimentally show that a 35-K preheating of the mirror assembly compensates for an absorbed laser power of 1.25 W. Therefore, the novel compensation regime "compound loading" for the suppression of laser-induced deformations is developed and proven. [DOI: 10.1117/1.JMM.12.1.013016]

Subject terms: deformable mirror; unimorph; laser-induced deformation; thermally-induced deformation; homogeneous loading; compound loading.

Paper 12084P received Nov. 15, 2012; revised manuscript received Feb. 8, 2013; accepted for publication Feb. 26, 2013; published online Mar. 13, 2013.

1 Introduction

The purpose of this study is the examination and optimization of the thermomechanical behavior of noncooled screen-printed unimorph deformable mirrors (DM) that are generally used for compensation for wavefront aberrations. The DM setup consists of a substrate with a reflecting surface on its front and a piezoceramic layer sandwiched between common and addressing electrodes on its rear surface. The application of an electric field between the common and addressing electrodes forces the piezoceramic layer to expand along the electric field direction and contract along the lateral direction as the piezoceramic material is poled along the field direction. Because the piezoceramic layer and the substrate are joined together, the mirror surface changes its shape. This established setup has been known for many years[1,2] and is referred to as a unimorph setup in this paper, as only one layer is active. DMs are integrated in an adaptive optical system where an aberrated wavefront is reflected on the DM surface in such a way that the DM introduces a wavefront aberration–opposed optical path length difference, compensating for wavefront aberrations from plane reference wavefronts.[3,4]

Wavefront aberrations in laser systems can be generated by thermal lensing; the absorption of laser power in the optical components of the laser system causes an increase in temperature, and thus, a corresponding gradient in the optical components. This temperature increase induces shape variations in the optical components, thereby changing their optical characteristics. Furthermore, the temperature increase changes the refractive index of the transmissive optical components owing to its temperature dependence. Both effects result in unwanted optical path length differences over the optical aperture. Thermally-generated optical phase length differences degrade the laser wavefront and the laser beam quality. These unwanted laser-power-induced changes cause the focus position to shift. In addition, the spot size of the laser beam is increased, and simultaneously the laser power density decreases.

The challenge of DM applications in high-power laser systems arises due to the laser-induced deformations of their surface. The mirror surface absorbs a fraction of the laser radiation, and the mirror temperature increases depending on the optical coating and the heat dissipation capability of the substrate material used. Thermal lensing establishes in the DM itself. This case is referred to as nonhomogeneous loading of a DM.

Homogeneous (temperature) loading of DMs is caused by environmental conditions during storage or operation. An ambient temperature increase during storage can cause reversible or irreversible mirror shape variations. Reversible

variations include temperature-induced bowing of the mirror substrate. They become irreversible if the thermally-generated bow and stress is too large and layers delaminate from the substrate, or the mirror breaks. Other reasons of irreversible bowing include temperature-induced changes in material properties or thermally-induced shrinkage. Thermally-induced shrinkage, such as that due to post-curing of adhesives in the mirror assembly, can induce permanent mirror shape variations. An ambient temperature increase during operation (and thus the mirror bowing) changes the active mirror properties. Hence, an originally flat mirror focuses or defocuses laser beams.

Compensation for thermal homogeneously generated and thermal nonhomogeneously generated deformations of the mirror surface by active leveling of the piezoelectric actuators decreases the mirror's operating range. Therefore, a primary objective of deformable-mirror developments is to minimize the changes in the mirror membrane by nonhomogeneous and homogeneous temperature loading.

Besides the introduced unimorph setup, other DM setups exist.[3,5] These days, electrostatically activated mirrors[6,7] and electromagnetically activated mirrors[8,9] are especially popular. The advantages of these mirrors include their great actuating capabilities, the facility of using a large number of actuators, and their manufacturing based on batch-fabrication; however, their thin deformed mirror membranes make the application in high-power laser systems difficult owing to the challenge of low stress application of high-power coatings and low heat dissipation within the membrane. Nevertheless, occasional examples of intracavity laser application have been given.[10] In contrast, piezoelectrically activated DMs are widespread in the field of laser beam shaping.[11–13] From their inception, unimorph (and bimorph) DMs have been applied to the compensation for thermal lensing,[14,15] and this is still the case. These days, unimorph and bimorph DMs with customized mirror coatings, mirror substrates, and actuating designs are commercially available from different companies, e.g., Cilas, TURN, and Active Optics NightN, but their thermomechanical design is not very sophisticated; in the case of homogeneous loading, by default, the differences in thermal expansion between substrate and piezoelectric layers are minimized, thereby minimizing the bimetal effect of the active mirror and leading to an athermal mirror design. Practical realizations of athermal designs result in glued lead zirconate titanate (PZT) disks on BK10 glass or Pyrex substrates.[16,17] Another practical realization exclusively uses piezoelectric disks glued together and polished to optical quality.[18] An alternative athermal setup is the application of a piezoelectric layer on thermally adapted metal. Suitable metals (with a coefficient of thermal expansion (CTE) around $7 \times 10^{-6}\,\mathrm{K}^{-1}$) include titanium, AlSi70, W80Cu20, Mo80Cu20, and W85Cu15 with corresponding thermal conductivities of 7.6, 120, 248, 165, and $162\,\mathrm{W\,m}^{-1}\,\mathrm{K}^{-1}$, respectively. These metal-based substrates are not popularly used, as their manufacturing and finishing leads to increased labor costs compared with those of glass substrates. The presented athermal approaches neglect the use of the metallization layer of the piezoelectric elements as well as the joining layer because they are much thinner than piezoelectric elements and mirror substrates in relative terms. Moreover, manufacture-imposed variations of the CTE of the piezoelectric layer, which generates a bimetal effect with the substrate, are widespread and tremendously challenging, and thus the athermal design is no longer valid.

Nonhomogeneous loading by a laser load changes the thermal mirror requirements as a fraction of the laser load is absorbed. The use of an athermal design approach would be possible in this scenario, as a temperature increase in the mirror assembly would (theoretically) not lead to a bimetal effect. Nevertheless, a large temperature increase in the mirror assembly is a serious drawback that can lead to device failure. Mirrors that can withstand high (laser) power preferably have a (dielectric) coating to decrease the power absorption. A high mirror temperature increase in the range of tens of Kelvins can lead to coating delamination and destruction. The stress distribution caused by the radial temperature profile can also lead to substrate delamination and breakage. The interface between the substrate and the active layer (adhesive joint) might postcure, thereby inducing permanent mirror deformation or delamination. Another aspect is the temperature-dependent thermomechanical material properties of the single layers, and thus, the discarding of the athermal approach. Moreover, the piezoelectric properties are temperature-dependent, and depolarization of the piezoelectric layer would lead to mirror malfunction. The laserpower-generated heat has to be dissipated and removed. The contemporary solution is the usage of a high heat dissipation substrate, e.g., copper, that is bonded with the active (piezoelectric) layer. The heat dissipation of the substrate can be increased further with the application of copper substrates with cooling channels.

However, state-of-the-art thermomechanical DM design for laser loading analyzes the mirror response upon homogeneous loading. Little work has been done on the nonhomogeneous thermal loading by laser and the interplay between homogeneous and nonhomogeneous thermal loading of DMs.

To answer this question, finite element analysis is carried out to optimize a multimaterial-based DM setup. The multimaterial approach integrates (stacks) certain layers with thermomechanical parameters that differ from the substrate and the piezoelectric active layer into the mirror setup. Therefore, the thermally induced strains in the single layers of the multilayer system are scaled by the layer thickness, thereby controlling the thermally induced bowing of the mirror surface.[19]

2 Mirror Design

2.1 *Deformable Mirror Setup*

The proposed DM is classified as a unimorph DM. The mirror substrate is a cylindrical low-temperature cofired ceramic (LTCC) membrane with a thickness of 200 μm and a diameter of 34 mm. A 600-μm-thick LTCC annulus frame reinforces the membrane's cylinder wall. This DM substrate offers 100-μm-thick screen-printed piezoelectric and 10-μm-thick functional (electrodes, insulation) layers on its rear surface. The front surface of the substrate's frame is annularly affixed to the mirror mount. A thick copper layer covers the membrane's front surface and the mirror mount. This layer is machined to optical quality and equipped with a functional coating [Fig. 1(f)].

2.2 *Hybrid Mirror Fabrication*

Conventional unimorph DM manufacturing uses piezoceramic discs affixed to a glass substrate that is subsequently

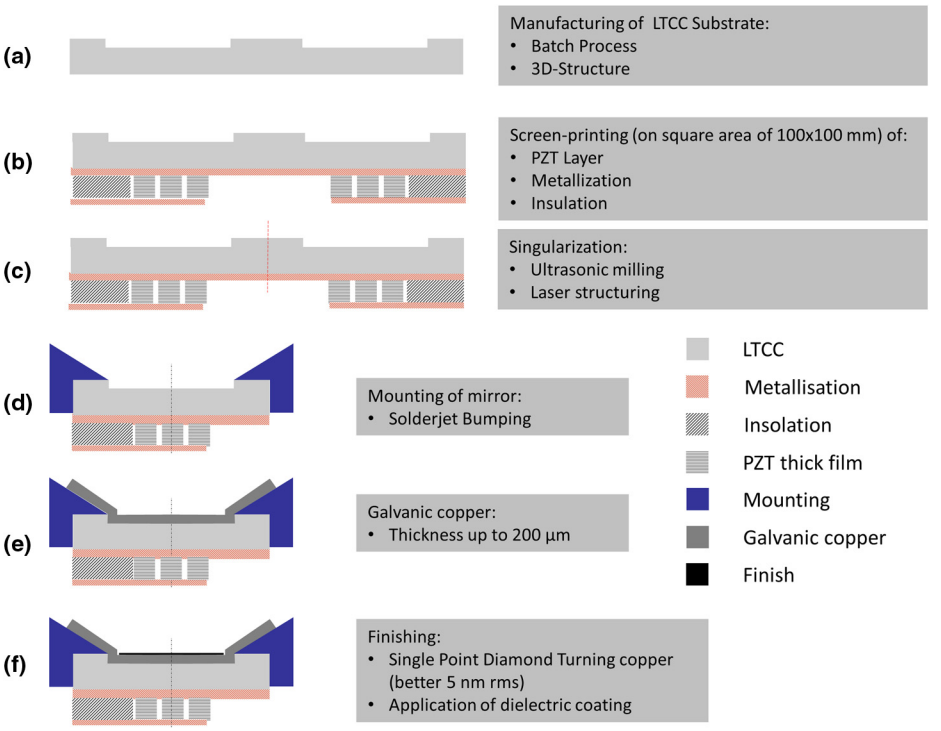

Fig. 1 Mirror manufacturing concept comprising six steps (a)–(f). Schematic shows the cross-section of a mirror membrane.

machined to optical quality, e.g., by manual glass polishing processes. Moreover, electrical wiring is very elaborate, as each discrete actuator is (manually) contacted and application side increases the demanded number of actuators. Therefore, the conventional approach has limitations in size and labor costs. In contrast, micro-opto-electro-mechanical systems (MOEMS) DM technologies rely on batch-fabrication to integrate actuators and their electrical wiring, and optical quality of the mirrors' surface is inherently comprised in the substrates. Thus limitations in size and cost per actuator are considerably decreased.

Therefore, we propose hybrid fabrication of unimorph MOEMS DMs, to overcome the drawbacks of conventional manufacturing. The developed process is based on ceramic printed circuit boards (PCB), thick films on ceramic substrates, and (conventional) optics manufacturing. It consists of six steps as shown in Fig. 1, of which two are (ceramic) batch-fabrication techniques and four are related to conventional optics manufacturing.

The batch-fabrication of the substrate is the first step necessary. The substrate material is made of multilayered LTCC (DuPont 951) that is fabricated by laminating single green sheets. These green sheets consist of a mixture of glass, ceramic, and organic additives and are thus very flexible. The single sheets are laminated together to form a stack before being sintered to a monolithic substrate at 850°C. Within the stack, both the membrane and its reinforcements (setup by additional annular LTCC layers) are integrated, the second serving as mounting aid structure, thereby simplifying handling and mounting as they absorb mechanical stress.

In the second step, the piezoceramic thick film actuator structures are applied onto the rear surface of the substrate. By using the screen-printing process, different DM actuator layouts with complex element patterns can be printed onto one substrate in one batch.

In the third manufacturing step, the mirrors are singularized by ultrasonic milling. The singularized mirrors are affixed to the mirror mount in the fourth step. The substrate's reinforcement is soldered with the mount by Solderjet Bumping. In Solderjet Bumping, the connecting parts are joined by a solder bump that is filled into a conical joining geometry of the mirror mount. The mount's conical joining geometries have a central bore, providing access of the solder to both mount and mirror. Thus, the mirror substrate and mount are form-locked and tightly connected. A design with 24 mechanical fixing joints is chosen to guarantee reliable mounting conditions and good thermal conductivity.

In the fifth step, thick-film copper metallization is carried out by electroplating. As the LTCC membrane is fixed by its reinforcements onto the mount, the copper metallization is electroplated onto the LTCC's front surface and onto the mirror mount to ensure a rigid joint and optimum heat dissipation of the mirror.

In the sixth step, the mirror surface is finished by means of single-point diamond turning (SPDT) of the copper thick film; electroplating and machining are carried out after mounting of the DM. Therefore, the mirror shape remains stable after machining, as no additional stress is induced in the mirror membrane through the mounting process. This results in excellent mirror surface quality and high reflectivity. The reflective surface may subsequently be coated.

2.3 *Simulations*

Very few studies have focused on DMs with screen-printed actuator layers[20,21] and, to the authors' knowledge, neither simulations nor measurements of the thermal behavior of the DM systems are available. In this section, extensive finite element method (FEM) simulations with different

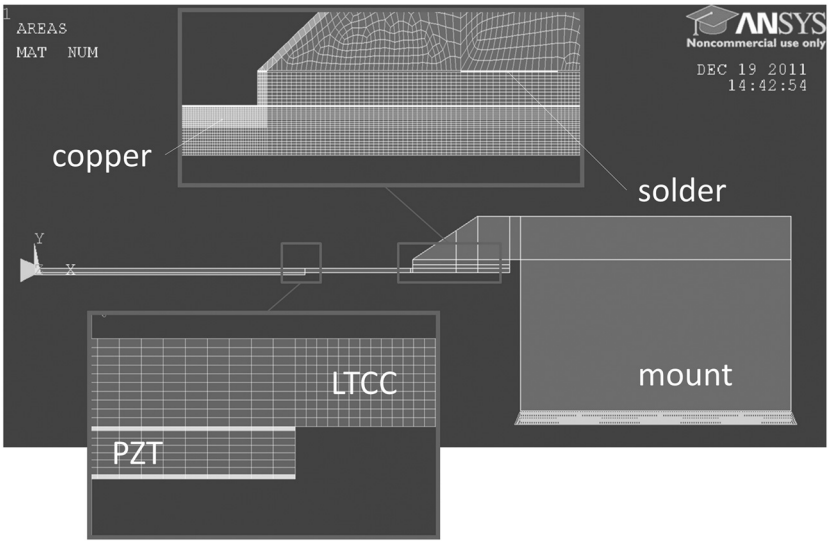

Fig. 2 Axisymmetric model of the deformable mirror (DM) setup with mount. Detail views show the element mesh.

copper-layer thicknesses are used to evaluate the DM response upon different thermal loading.

The simulation model of the DM, and its mechanical boundary conditions, are shown in Fig. 2. The assembly consists of an LTCC mirror substrate, a PZT layer with sandwiching gold electrodes, solder, and a copper layer grown onto both the LTCC membrane and the metallic mount. The mirror substrate is joined with the mount that has 24 conical joining geometries equally spaced on a diameter of 40 mm. The conical joining geometries have bores of 1 mm in diameter, and they are placed onto the reinforcing frame and filled with solder bumps. This geometry is simplified in the simulation and replaced by a 1-mm-wide, 10-μm-thick solder layer (X22CrNi17) between the mount and mirror substrate. The movement of the center of the model (mirror membrane) is suppressed along the x direction, and the mount's bottom area of support is allowed to radially expand. Figure 2 shows the cross-section of the model for a simplified representation. The detail views show the element mesh.

All simulations are based on ANSYS Multiphysics 11.0. The ANSYS program uses the element type "plane 223" for all elements and materials. The element's degree of freedom is set to structural-thermal with a weak (load vector) coupling and axisymmetric element behavior.

The first set of simulations examines the influence of mount material and copper-layer thickness upon thermally induced deflection of the mirror surface (homogeneous loading). These investigations serve for the determination of suitable mount materials and the influence of copper-layer thickness on the thermally induced deflection. Next, the influence of mount material and copper-layer thickness on the laser-induced temperature change and deflection of the mirror is evaluated (nonhomogeneous loading). Additionally, the interplay between homogeneous and nonhomogeneous loading of the mirror setup is analyzed.

2.4 *Homogeneous Loading*

The first simulation step calculates the thermally induced bowing for a large-deflection static analysis of the mirror setup. Temperatures of 30 K are applied to all the mirror nodes, and the stress matrix is calculated. The shape variation of the mirror is analyzed for copper-layer thicknesses of 150, 200, and 225 μm for different mount materials. The following mount materials are investigated: Invar (Fe65Ni35), Kovar (Fe–Ni–Co alloy), copper (Cu), W85Cu15 (WCu), and CE7 (Si70Al30). Copper is chosen because it has good thermal conductivity and a large CTE value. In contrast, the CTE of Invar is very low. The materials W85Cu15, Kovar, and CE7 are considered because they have CTEs similar to that of LTCC with $5.8 \times 10^{-6}\,\mathrm{K}^{-1}$. The mount materials exhibit CTEs between 1.7×10^{-6} and $23.8 \times 10^{-6}\,\mathrm{K}^{-1}$.

Figure 3 shows the simulated peak-to-valley (P-V) membrane deflections in dependence on the mount material. The CTE of the mount material is also integrated in Fig. 3 as a bar diagram with reference to the secondary axis of ordinate. In particular, Invar (CTE $= 1.7 \times 10^{-6}\,\mathrm{K}^{-1}$) causes large membrane deformations due to its strong CTE mismatch compared to the CTE of the mirror substrate. The insensitivity of the membrane deflection with copper-layer thickness variations increases with the CTE values of the mounts. Kovar has a CTE ($5.8 \times 10^{-6}\,\mathrm{K}^{-1}$) that is compatible with that of LTCC; however, it causes large P-V membrane deflections between -10 and -15 μm. Further, Kovar also shows a

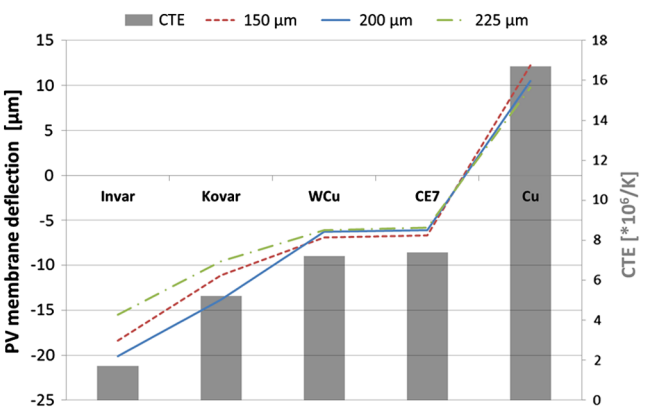

Fig. 3 Thermally-induced peak-to-valley (P-V) mirror deformation for different mount materials.

considerable dependence on the copper-layer thickness. A copper (CTE $= 16.7 \times 10^{-6}\,\mathrm{K}^{-1}$) mount matches the CTE of the thick copper metallization; however, it shows a membrane deflection between 9 and 13 μm.

The materials W85Cu15 and CE7 exhibit CTEs of 7.2×10^{-6} and $7.4 \times 10^{-6}\,\mathrm{K}^{-1}$, respectively, and they show the lowest deflection and dependence on copper-layer thickness variations. The CE7 material shows identical thermally induced deflection ($0.2\ \mu\mathrm{m\,K}^{-1}$) for thicknesses of 225 and 150 μm. In contrast, for W85Cu15, the deflection decreases with increasing copper-layer thickness. This behavior could be explained by the larger Young's modulus of W85Cu15 compared with that of CE7. The simulation results also indicate the availability of a mount material with a CTE between 9×10^{-6} and $11 \times 10^{-6}\,\mathrm{K}^{-1}$, for which there is no P-V membrane deformation introduced. These mount materials include CE9 (AlSi60), W72Cu28, and CE11 (AlSi50).

2.5 *Nonhomogeneous Loading*

The nonhomogeneous loading of a DM is caused by laser beams that show an intensity distribution that varies with the distance r to the propagation axis. Beams that are mostly used in lasers can be considered as Gaussian beams. Gaussian beams have transverse electric fields and an intensity distribution $I(r)$ over its beam diameter ω that is well approximated by the following Gaussian function:

$$I(r) = I_o\left(\frac{\omega_o}{\omega_r}\right)^2 \exp^{\left(\frac{-2r^2}{r^2}\right)} = A * \exp^{\left(\frac{-2r^2}{r^2}\right)}. \quad (1)$$

The Gaussian-shaped intensity distribution implies a nonhomogeneous absorption, and it induces a nonhomogeneous temperature distribution in the mirror membrane. The thermally induced changes by nonhomogeneous loading are evaluated by simulations that implement a Gaussian-shaped heat flux. The heat flux is applied to the copper surface (line) of the mirror with a beam radius of 1 cm (corresponding to a correctable laser beam with a diameter of 2 cm). The movement of the center of the axisymmetric model is suppressed along the x direction, and the mount's bottom area of support is allowed to move radially. The temperature at the mount's bottom area is maintained constant.

Figure 4 shows the Gaussian heat flux and the model's cross-section (instead of the axisymmetric simulation model). The temperature change is evaluated at three points that are also marked in the figure. Point 1 is located on the copper surface and at the mirror center, and point 2 is located on the radius of the piezoceramic layer and at the mirror center. Point 3 is on the radius of the solder joint on the surface of the deposited copper. This point would be a practical measurement point for a hand-held thermocouple unit that can monitor the temperature changes in the mirror assembly.

Next, we investigate the impact of mount materials and copper-layer thickness on the nonhomogeneously generated thermal changes. The mount materials are CE7, CE11, and W85Cu15. The investigated copper-layer thicknesses are 100, 150, 200, and 225 μm. The term A in Eq. (1) is scaled down until the heat flow is 1 W for every value of the copper-layer thickness. Surface convection effects are not taken into account, as the maximum temperature increase is <10 K.

We evaluate the static mirror deformation and the temperature increase at the characteristic points 1, 2, and 3 of the mirror assembly. Figure 5 depicts the heatflux-induced deformation at measurement point 1. The deformation decreases (linearly) with the copper-layer thickness from 2.5 to 1.3 $\mu\mathrm{m\,W}^{-1}$ for 100 and 200 μm, respectively. Thus, one can deduce the insensitivity of the mount material on the laser-induced deformation. Therefore, the following analysis of the simulation results is made solely for the CE7 mount material.

The temperature increases at measurement point 1 are 5.3, 3.8, and 3.0 K for 100, 150, and 200 μm, respectively (Fig. 6). These temperature changes are moderate; they are not critical for depolarization of the piezoceramic element to occur. The laser-induced temperature changes at measurement points 2 and 3 are also of note (see Fig. 6). The simulations reveal a temperature decrease with mirror radius and copper-layer thickness. Measurement point 2 shows only a temperature increase between 1.3 and 1.9 K for 200 and 100 μm, respectively. The temperature increase at the mirror mount is very small, and it is between 0.8 and 1.0 K for 200 and 100 μm, respectively. These changes are in the range of the measurement-resolution temperature-monitoring devices such as handheld thermocouple units. The maximum temperature increase occurs at the mirror center, as the highest flux (laser intensity) is centered there as the absorbed power is dissipated mainly by the copper layer. The thermal

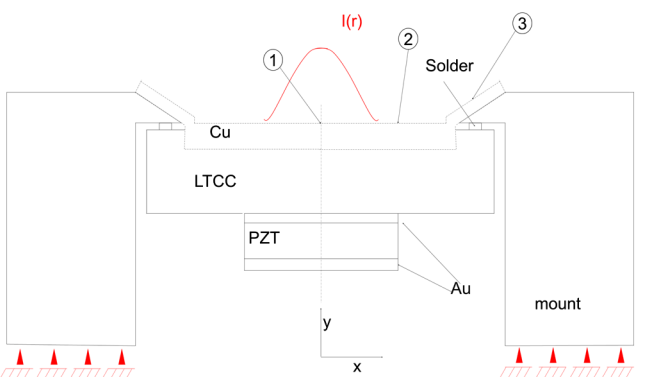

Fig. 4 Simulation model of nonhomogeneous loading with measurement points 1–3 (not to scale).

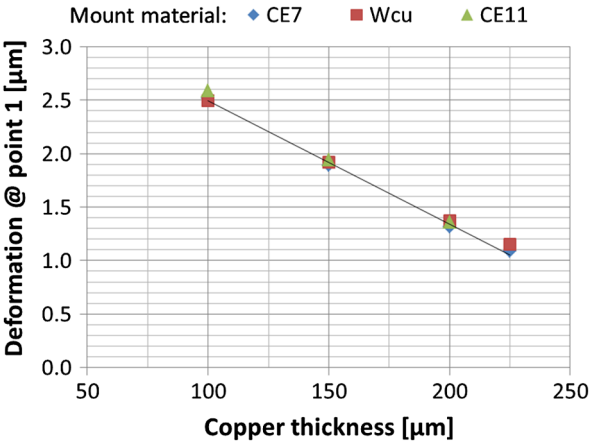

Fig. 5 Induced deformation at measurement point 1 for different mount materials.

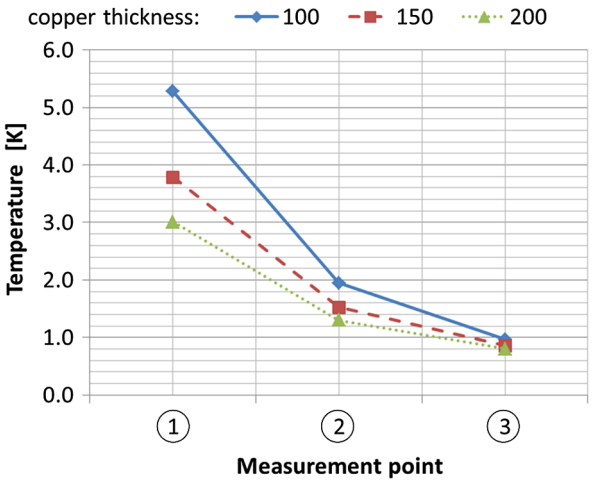

Fig. 6 Simulated temperature increase on measurement points 1–3.

conductivity of the mount material plays a subordinate role in heat dissipation.

2.6 *Compound Loading*

The simulations reveal a novel possibility of compensation for laser-generated mirror deformation by homogeneous-thermal-loading-imposed mirror deformation. The tailoring of the thickness of the large CTE front surface layer leads to the tailoring of the thermally-induced deflection by homogeneous loading. The homogeneous loading of the optimized design with 200-μm copper-layer thickness results in a thermally induced deflection with a rate of $-0.2\ \mu\mathrm{m}°\mathrm{C}^{-1}$, whereas a laser loading causes a deflection with a rate of $1.3\ \mu\mathrm{m\,W}^{-1}$. Therefore, a 40-K temperature increase of the mirror assembly results in -8-μm P-V membrane deformation that can compensate for an absorbed power of 6 W ($1.3\ \mu\mathrm{m\,W}^{-1} \times 6\,\mathrm{W} = 7.8\ \mu\mathrm{m}$). This novel approach of specific loading is defined as compound loading and shall be reviewed as part of this work.

2.7 *Material Selection and Mirror Fabrication*

The presented mirror design was developed to achieve two objectives: the development of a mirror setup that realizes the multimaterial approach and the development of mirror's hybrid fabrication technology. This is particularly important to reduce the fabrication cost of the mirror and thereby open up applications.

The multimaterial approach requires a special designed layer setup and allows control of the thermally induced bowing of the mirror surface (depending on the thermal load).[19] In particular, three decisions of material selection and its relation to device design optimization and manufacturing are worth discussing: the application of LTCC substrates, screen-printed piezoceramic layers, and electroplated copper thick-film.

LTCC has been industrially established for manufacturing of medium- and high-volume production of multilayer electronic substrates. LTCC green sheets are available in standard sizes of up to 6×6 and 8.75×8.75 inches, respectively. LTCC allows for 3-D electrical connection as well as integration of resistors, capacitors, and inductors in one compact ceramic substrate. Channels as well as membranes can be easily incorporated into the multilayer setup. Moreover, LTCC is characterized by its robustness and reliability. It has been chosen because of its compatibility to the screen-printed piezoceramic actuator structures.

We use a piezoceramic thick film paste IKTS PZ-5100 based on PZT. Although intensive research in the field of lead-free piezoelectric materials to replace PZT ceramics has gained tremendous progress during the last 10 years, piezoelectric performance and working temperature range are still unsatisfactory for high-performance actuator applications. Furthermore, lead-free piezoceramic thick film pastes have been proven for ultrasonic transducer applications but show weak actuator properties.

Screen-printing is a widespread technique in the manufacturing of thick-film hybrid electrical microsystems. Standard equipment is suitable for processing of piezoceramic thick-film paste IKTS PZ-5100 and has already been shown on 5-inch substrates. This technique enables reduction of the DM costs of fabricating complex actuator layouts and their electrical wiring. Commonly applied assembling techniques such as gluing or soldering of piezoceramic parts onto mirror substrates fail as actuator patterns become more complex and device structures are miniaturized. Processing steps of cutting, polishing, placing, and fixing of piezoceramic components become very laborious and time- and cost-consuming as feature size decreases. Dimensions of the manufactured parts are limited and constrained to simple shapes like discs, plates, rings, cylinders, etc.[22] Moreover, stability of interface between microelectronic substrate and piezoceramic part depends on the interface material, e.g., glue or solder. Deposition of polymer-based glues can lead to reduced temperature and chemical stability. For applications under vacuum, outgassing of interface ingredients can play a role. Also, reliable connection to the piezoceramic part has to be solved. Here, the piezoceramic layer is sintered and joined to the substrate, thereby creating a strong interface with a high-temperature working range and potentially low outgassing.

The deposition of copper by electroplating SurTec865 results in mirror bases with leveled, ductile and low-stressed copper layers. Furthermore, electroplating of SurTec865 at 28°C is an economical process with low maintenance cost. Therewith, metallization layer with large (about 100 μm) and exact layer thickness can be deposed. The copper layer offers excellent machinability by SPDT, an ultra-precision diamond turning process that result in surfaces with optical quality. Its optical quality is mandatory for DM's successful application in optical systems. Besides the economic reasons, thermomechanical characteristics are reasonable as well. First, copper's large thermal conductivity is used to transmit laser-induced heat from the mirror center to mirror mount, to prevent excessive heating of the membrane. Second, the CTE of copper differs significantly from those of LTCC and PZT. This is explicitly intended for application of the multimaterial approach; as shown, by scaling the copper-layer thickness, the compensation of laser-induced deformations of the mirror membrane is possible through heating of the DM (compound loading). The multimaterial approach especially relies on the mismatch of thermal expansion between the different layers. In this context it is particularly essential that the copper layer deposition is carried out at 28°C to avoid thermally induced stresses caused by

the electroplating process. For that reason, the material combination of copper, LTCC, and PZT is very suitable, especially along with the reliable and economic material deposition by electroplating and screen-printing.

3 Experimental Verification of the MOEMS Deformable Mirror

3.1 *Adaptive Optical Measurement Setup*

The adaptive optical measurement setup consists of a collimated laser diode emitting laser radiation at 532 nm. The laser beam is expanded to 25.7 mm and reflected by the DM. A beam-splitter cube directs the beam to a Shack–Hartmann wave front sensor (WFS), and a second beam expander compresses the beam to the WFS aperture. The WFS (SHSLAB-HR-130-FW; Optocraft) has a dynamic range of 420 μm, a repeatability of 2.1 to 3.2 nm, and a measurement accuracy of 50 nm. The measurement plane of the WFS is conjugated to the DM plane, thereby ensuring absolute wavefront measurement. The data from the WFS are analyzed using SHSWorks software (Optocraft GmbH) and subsequently processed with LabVIEW (National Instruments). LabVIEW also samples the measurement of the mirror temperature and controls voltage of the piezoceramic actuators and power of the Peltier element. A Peltier element is integrated in the mirror mount and is controlled by a laboratory power supply unit. It works in a LabVIEW-generated closed loop with a temperature sensor (digital thermometer HH506-RA, Omega) that is placed very close to the mirror membrane at one of the solder joints on the mount. The Peltier element is used for evaluation of the mirror response upon homogeneous loading and compound loading.

The high-power laser beam for the nonhomogeneous loading (beam diameter 20 mm) is incident on the DM at a small angle with reference to the normal of the mirror surface. Thus, the diameter remains constant and is not elliptically deformed. The power of the reflected beam is measured by a power meter. The high-power laser (JenLas® fiber cw 400) emits radiation at 1070 ± 10 nm and has an output power up to 400 W. The laser can be operated in the continuous-wave (cw) mode or modulated at a 100-kHz repetition rate. The M^2 value is better than 1.1, and its polarization is random. The high-power laser is used with an isolator. The nonhomogeneous loading of the DM is performed in three stages by varying the duty cycle. The duty cycle is maintained constant at 5%, 50%, and 100%, and the laser power is varied.

3.2 *Measurement Results*

3.2.1 *Optical quality*

The optical surface of the mirror is cut spherical with a radius of 2.5 m by the diamond-turning process. The adaptive optical measurement setup analyzes the surface (optical quality) of the fabricated deformable MOEMS mirror, and the measurements reveal a deviation from spherical shape of 1.4 μm upon neglecting the Zernike polynomials piston, tip/tilt, and defocus. The application of the piezoelectric actuators with up to $\pm$20% of their stroke decreases the deviation to 80 nm rms for a mirror aperture of 20.8 mm.

3.2.2 *Homogeneous loading*

The WFS analyzes the P-V mirror–membrane deformation for homogeneous heating. Measurements of the P-V membrane deformation are also made by the Tencor FLX-2320 measurement system. Both measurements are done with short-circuiting of electrodes, and the results are shown in Fig. 7. The P-V of the mirror membrane increases linearly at a rate of -0.12 μm°C^{-1} between 26°C and 56°C; this value is consistent with both measurement systems.

Athermal design examples regarding the mirror response under homogeneous loading show similar results; thermal stability tests of unimorph DMs (glass substrate) over a small temperature range (from 13°C to 25°C) show a linear membrane deformation of 0.11 μm°C^{-1} (P-V).[23] Similar results of 0.11 μm°C^{-1} were recently published for BK10 substrates and larger temperature ranges between 0°C and 55°C.[24] Other measurements reveal a change of 0.34 μm°C^{-1} due to defocus upon homogeneous loading between 17°C and 23°C and a glass substrate.[25] A mirror with Pyrex substrate shows a P-V deformation of -0.12 μm°C^{-1} over a temperature range of 30°C to 45°C.[16] All the relevant previous studies have reported that defocus is the major component under homogeneous loading. Comparison of the developed multilayer design with the state-of-the-art athermal mirror designs reveals a comparable thermally induced deflection.

3.2.3 *Nonhomogeneous loading*

The mirror membrane response to different laser loads is measured, and the P-V deformation is evaluated. The applied cw laser load results in absorbed power values between 500 mW and 2.1 W. The absorbed power is calculated by the incident power and the reflectivity (98%) of the mirror surface, neglecting transmission and light scattering. The results are shown in Fig. 8. The P-V deformation increases linearly with increasing values of absorbed power, and it reaches a value of 8 μm for an absorbed power of 2.1 W. The rate of the P-V membrane deformation under nonhomogeneous loading is 3.4 μm W^{-1}. The mirror membrane bends upward with increasing power absorption, thereby indicating the defocusing of a parallel beam.

3.2.4 *Compound loading*

The induced mirror membrane bending for homogeneous loads is opposite to that under nonhomogeneous thermal

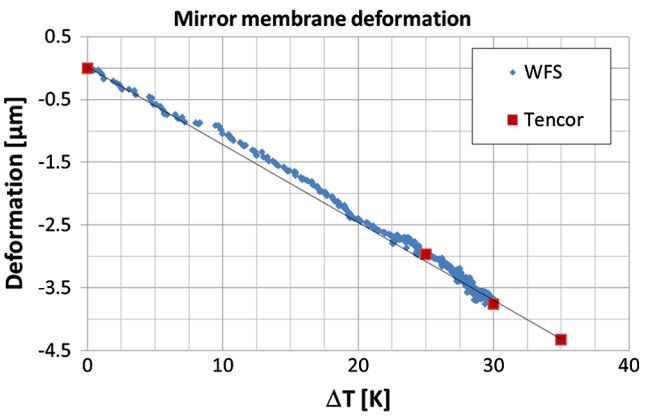

Fig. 7 Temperature-induced P-V deflection of the mirror membrane. Slope of the linear fit is -0.1 μm K^{-1}.

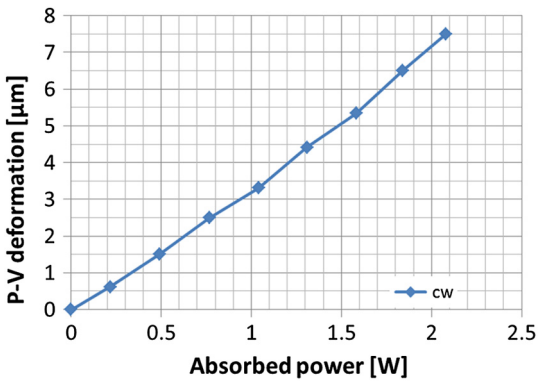

Fig. 8 Plot of the absorbed power against the P-V deformation. The laserload–induced membrane deformation is 3.4 μm W^{-1}.

loads. A homogeneous load induces focusing of the mirror, whereas a nonhomogeneous load induces defocusing of the mirror. This suggests the possibility of the precompensation of laser-induced deformations by heating of the DM (compound loading). Two sets of compound loading measurements [Fig. 9(a) and 9(b)] are carried out in order to prove this approach; these measurements evaluate the thermally induced P-V mirror deflection and the change in defocus.

Figure 9 shows the measured P-V mirror membrane deformation induced by the absorbed power for different homogeneous preloadings along with the reference behavior in the absence of preloading. In the absence of homogeneous preloading, the P-V mirror membrane deformation again increases linearly at a rate of 3.4 μm W^{-1}. This behavior changes according to the homogeneous preloading of the mirror. A preheating of 16 K (to 35°C) increases the P-V mirror deformation to 2.6 and 1.7 μm for Fig. 9(a) and 9(b), respectively, in the absence of high-power laser loading. An increase in absorbed power decreases the P-V mirror membrane deformation to a minimum at around 0.5 W for both measurements. With further increase of the absorbed power, the P-V mirror membrane deformation again increases. A polynomial trend line (of the third power) fits these characteristics.

A similar behavior is observed for every preheating temperature for both sets of measurements. The maximum P-V membrane deformation occurs at a maximum absorbed power of 2.3 W. Furthermore, the deformation decreases with homogeneous preheating. In addition, the measurements show a minimum P-V membrane deformation of 1.1, 1.7, and 2 μm for homogeneous loadings of 16, 25, and 35 K, respectively. The minimum values are comparable for both measurements Fig. 10(a) and 10(b), and they define the optimum compound loading.

Defocusing is used as figure of merit for evaluating the precompensating properties. Figure 10 shows the defocus values for measurements Fig. 10(a) and 10(b) under compound loading. Nonhomogeneous heating without homogeneous loading induces a negative defocus (represented by C_3). The homogeneous preloading increases the defocus in the absence of power absorption. The defocus increases linearly down to negative defocusing with increasing power absorption. The measurements reveal the compensation of the nonhomogeneously generated defocus by homogeneous loading. Measurement [Fig. 10(a)] suggests the ability to compensate for the defocus induced by 1.25 W of absorbed power by 34 K of homogeneous loading. Measurement [Fig. 10(b)] suggests a compensation of <1 W for a comparable homogeneous loading of 35 K.

The range of the piezoelectric actuators also is measured at optimum compound loading for an electric field of 2 kV/mm that is applied to all the actuators. Here, the piezoelectric actuators result in a P-V membrane deformation of 14.8 μm and minimum defocus C_3 of −6.7. This stroke can be used for the compensation of thermal lensing in the optical system, residual membrane deformation at optimum compound loading, and residuals due to manufacturing.

3.3 *Comparison with Simulated Values*

The simulations reveal a membrane deformation rate of −0.2 μm°C^{-1} and 1.3 μm W^{-1}. This corresponds to a

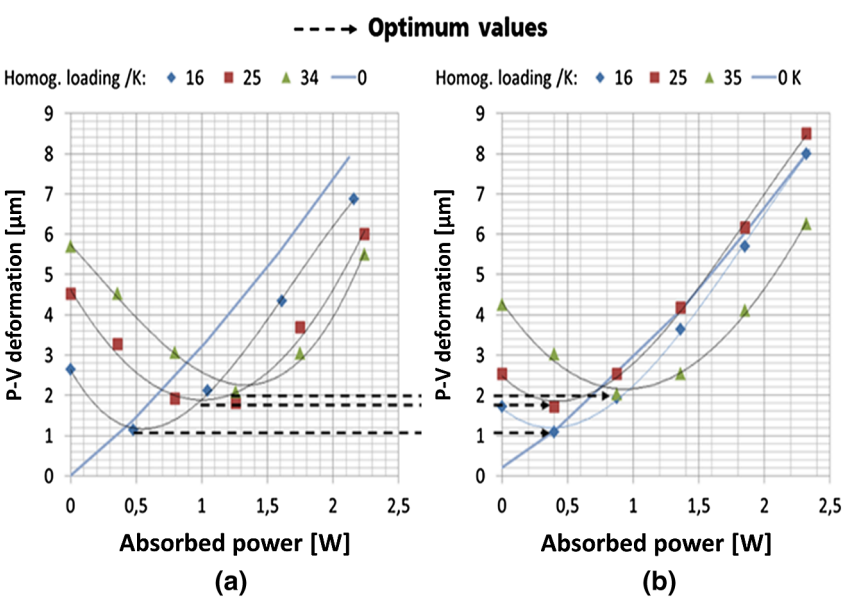

Fig. 9 P-V membrane deformation for two sets of measurements, (a) and (b). The measurements reveal an optimum homogeneous preheating for minimal membrane deformation.

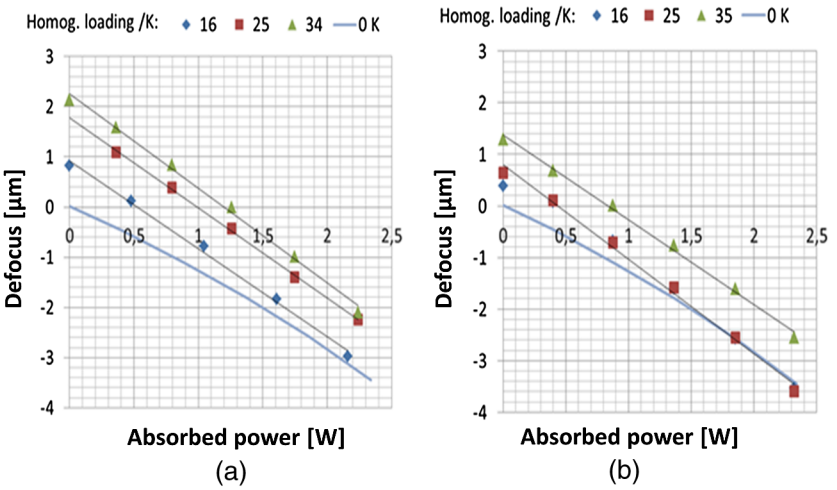

Fig. 10 Zernike coefficients of defocus in measurements (a) and (b). The measurements reveal an optimum homogeneous loading that compensates for the defocus term under different nonhomogeneous loads.

precompensation of 6 W by homogeneous heating of 40 K under the compound loading regime. An absorbed laser power of 6 W corresponds to a reflected laser load of 600 W for 1% absorption. In particular, high-power coatings enable a very high reflection of 99.9% and more, thereby corresponding to a reflected laser power of 6 kW. This shows the theoretical proof of concept for the suitability of the mirror for high-power applications.

The measurements show a lower membrane deformation rate of $-0.2\ \mu m°C^{-1}$ and a higher laser-induced deformation rate of $3.4\ \mu m\,W^{-1}$. Two main reasons are identified: the coating absorption might be higher than estimated and the heat dissipation capability of the mirror might be decreased. The copper layer contributes most to heat dissipation capability. We measure an approximately 35% lower electrical conductivity of the plated copper layer compared to bulk material. Therewith, we conclude a lower thermal conductivity of the copper layer that is proportional to its electrical conductivity (Wiedemann–Franz law). Future electroplating process optimization should increase copper's thermal conductivity.

4 Conclusions

Hybrid fabrication that is based on ceramic PCBs, thick films on ceramic substrates, and (conventional) optics manufacturing was developed and verified by MOEMS DMs. A multimaterial layer design was applied in the DM, leading to unique thermal mirror properties. Therewith, a method was developed and presented that compensates for laser-induced deformation of DM surfaces without the application of piezoceramic actuators.

Simulations are carried out for device optimization, showing that in the case of homogeneous loading, the deformation of the mirror surface depends on the mount material and copper-layer thickness, and can be scaled by tailoring of both. Further, the results indicate the availability of a mount material with a CTE between 9×10^{-6} and $11 \times 10^{-6}\ K^{-1}$, for which there is no P-V membrane deformation introduced by homogeneous loading. These mount materials include CE9 (AlSi60), W72Cu28, and CE11 (AlSi50). In the case of nonhomogeneous laser loading, the deformation of the mirror surface depends on the copper-layer thickness and not on the mount material. A homogeneous temperature increase (homogeneous loading) of the mirror setup counteracts laser-induced mirror deformation. It is experimentally shown that a 35-K preheating of the mirror assembly could compensate for an absorbed laser power of 1.25 W. The comparison between simulation and experimental results reveal a larger laser-induced mirror surface deformation than expected, which is attributed to the decreased thermal conductivity of the electroplated copper layer.

Acknowledgments

The authors thank the German Federal Ministry of Education and Research (BMBF) for their financial support within the project "Kompetenzdreieck Optische Mikrosysteme–KD OptiMi" (FKZ: 16SV5473). The authors furthermore thank S. Türke.

References

1. J. Feinleib, S. G. Lipson, and P. F. Cone, "Monolithic piezoelectric mirror for wavefront correction," *Appl. Phys. Lett.* **25**(5), 311–313 (1974).
2. E. Steinhaus and S. G. Lipson, "Bimorph piezoelectric flexible mirror," *J. Opt. Soc. Am.* **69**(3), 478–481 (1979).
3. R. K. Tyson, *Principles of Adaptive Optics*, Academic Press, New York (1991).
4. E. Hecht, *Optik*, 5th revised edition, Oldenbourg Verlag, München (2009).
5. R. H. Freeman and J. E. Pearson, "Deformable mirrors for all seasons and reasons," *Appl. Opt.* **21**(4), 580–588 (1982).
6. G. Vdovin and P. M. Sarro, "Flexible mirror micromachined in silicon," *Appl. Opt.* **34**(16), 2968–2972 (1995).
7. S. Bonora and L. Poletto, "Push-pull membrane mirrors for adaptive optics," *Opt. Express* **14**(25), 11935–11944 (2006).
8. R. Hamelinck et al., "Validation of a new adaptive deformable mirror concept," *Proc. SPIE* **7015**, 70150Q (2008).
9. ALPAO Adaptive Optics, Deformable mirrors, http://alpao.fr/products_deformable_mirrors.html (October 8 2011).
10. G. Vdovin and V. Kiyko, "Intracavity control of a 200-W continuous-wave Nd:YAG laser by a micromachined deformable mirror," *Opt. Lett.* **26**(11), 798–800 (2001).
11. A. A. Aleksandrov et al., "An adaptive optical system for controlling laser radiation," *J. Opt. Technol.* **74**(8), 550–554 (2007).
12. F. A. Starikov et al., "Correction of vortex laser beam in a closed-loop adaptive system with bimorph mirror," *Opt. Lett.* **34**(15), 2264–2266 (2009).
13. P. Wnuk, C. Radzewicz, and J. Krasinski, "Bimorph piezo deformable mirror for femtosecond pulse shaping," *Opt. Express* **13**(11), 4154–4159 (2005).

14. C. A. Primmerman and D. G. Fouche, "Thermal-blooming compensation: experimental observations using a deformable-mirror system," *Appl. Opt.* **15**(4), 990–995 (1976).
15. A. L. Rukosuev et al., "Adaptive optical system based on bimorph mirror and Shack-Hartmann wavefront sensor," *Proc. SPIE* **4493**, 261–268 (2002).
16. E. M. Ellis, "Low-cost bimorph mirrors in adaptive optics," PhD Thesis, Imperial College of Science, Technology and Medicine, University of London (1999).
17. S. Verpoort and U. Wittrock, "Unimorph deformable mirror for telescopes and laser applications in space," in *Proc. 8th Int. Conf. Space Opt.*, Rhodes Island, Greece (2010).
18. C. Schwartz, E. Ribak, and S. G. Lipson, "Bimorph adaptive mirrors and curvature sensing," *J. Opt. Soc. Am. A* **11**(2), 895–902 (1994).
19. C. Reinlein, "Thermomechanical design, realization and testing of screen-printed deformable mirrors," [in German], PhD TU-Ilmenau (2012).
20. T. R. Möller, *Ein Beitrag zur Untersuchung von Bimorphspiegeln für die Präzisionsoptik*, Aachen, Shaker (2002).
21. G. Rodrigues et al., "Modular bimorph mirrors for adaptive optics," *Opt. Eng.* **48**(3), 034001 (2009).
22. M. Kosec, "Processing of ferroelectric ceramic thick films," in *Multifunctional Polycrystalline Ferroelectric Materials: Processing and Properties*, L. Pardo and J. Ricote, Eds., Springer Series in Material Science, pp. 39–61, Springer, New York (2011).
23. Y. Ning et al., "Thermal stability test and analysis of a 20-actuator bimorph deformable mirror," *Chin. Phys. B* **18**(3), 1089–1095 (2009).
24. S. Verpoort, "Entwicklung neuartiger deformierbarer Spiegel für den Einsatz in Hochleistungslasern," PhD Thesis, Universität Duisburg-Essen (2011).
25. J. C. Dainty, A. V. Koryabin, and A. V. Kudryashov, "Low-order adaptive deformable mirror," *Appl. Opt.* **37**(21), 4663–4668 (1998).

Claudia Reinlein received her diploma degree in mechanical engineering from the Technical University in Ilmenau, in 2006. In 2012, she received her PhD degree from the Technical University in Ilmenau for her work on the development of screen-printed deformable mirrors. She is currently working as a researcher at Fraunhofer IOF in Jena, Germany where she is involved in research and development of deformable mirror technology.

Sylvia Gebhardt graduated from the Technical University Bergakademie Freiberg in 1996 with diploma degree in material science and technology. She was awarded a PhD in 2000 for her thesis on development and characterization of fine-scaled 1-3 piezocomposites for ultrasonic transducers. She is currently working as a senior research scientist at the Department of Smart Materials and Systems at Fraunhofer Institute for Ceramic Technologies and Systems, Dresden, Germany. Her research interests include piezoceramic components based on thick-films, multilayers, microstructures, and fibers and their integration into sensor-, actuator-, and ultrasonic transducer systems.

Ramona Eberhardt is the head of the department precision engineering at the Fraunhofer Institute of Applied Optics and Precision Engineering, Jena. She worked at the Friedrich Schiller University of Jena as a research assistant and scientist in the area of glass development and glass soldering technologies from 1982 to 1991. She also received her PhD degree in chemistry from the Friedrich Schiller University of Jena about investigations of thermo-optical properties of glass. From 1992 to 2004, she was a group manager of the micro assembly group at the Fraunhofer IOF, Jena. She heads the department precision engineering at the Fraunhofer IOF, since 2005. Her experiences especially include precision fixation technologies like soldering and adhesive bonding, material sciences, and packaging of opto-mechanical systems.

Andreas Tünnermann received the diploma and PhD degrees in physics from the University of Hannover in 1988 and 1992, respectively. In 1997, he received the habilitation. He was head of the department of development at the Laser Zentrum Hannover from 1992 to 1997. In the beginning of 1998, he joined the Friedrich-Schiller-University in Jena, Germany as a professor and director of the Institute of Applied Physics. In 2003, he was appointed as the director of the Fraunhofer Institute for Applied Optics and Precision Engineering IOF, in Jena. His main research interests include scientific and technical aspects associated with the tailoring of light. He is author of more than 400 papers in renowned international journals. He is a sought-after expert in optics and photonics industry. He is founder and member of the board of directors of the industry driven cluster Opto-Net Jena, one of the most dynamic regional optics clusters in Europe. His research activities on applied quantum electronics have been awarded e.g., with the Gottfried-Wilhelm-Leibniz-Award (2005). In 2013, he became a fellow of SPIE.

Biographies and photographs of the other authors are not available.